

# SUPPORTING INFORMATION

## Anti-Biofouling and Self-Cleaning Surfaces

### Featured with Magnetic Artificial Cilia

*Shuaizhong Zhang<sup>1,2</sup>, Pan Zuo<sup>1</sup>, Ye Wang<sup>1,2</sup>, Patrick Onck<sup>3</sup> and Jaap den Toonder<sup>1,2\*</sup>*

<sup>1</sup> Department of Mechanical Engineering, Eindhoven University of Technology, P.O. Box 513, 5600 MB Eindhoven, The Netherlands

<sup>2</sup> Institute for Complex Molecular Systems, Eindhoven University of Technology, The Netherlands

<sup>3</sup> Zernike Institute for Advanced Materials, University of Groningen, Groningen, The Netherlands

\* Corresponding author (E-mail: [j.m.j.d.toonder@tue.nl](mailto:j.m.j.d.toonder@tue.nl)).



## SI 1: Algae culturing – different algae strains

Five different strains of microalgae were cultured: (1) *Raphidocelis subcapitata*, (2) *Scenedesmus sp.*, (3) *Monoraphidium griffithii*, (4) *Scenedesmus quadricauda*, and (5) *Chlorella luteoviridis*. The culture medium for *Raphidocelis subcapitata* was EG:JM (see [https://www.ccap.ac.uk/media/documents/EG\\_JM.pdf](https://www.ccap.ac.uk/media/documents/EG_JM.pdf) for details). For the rest, the medium was 3NBBM+V (see [https://www.ccap.ac.uk/media/documents/3N\\_BBM\\_V.pdf](https://www.ccap.ac.uk/media/documents/3N_BBM_V.pdf) ). The home-built culturing system is shown in **Figure S1A**. The growth of these algae as a function of culture time is shown in Figure S1B. We chose *Scenedesmus sp.* for the experiments because they create fouling the fastest as shown in Figure S1C.

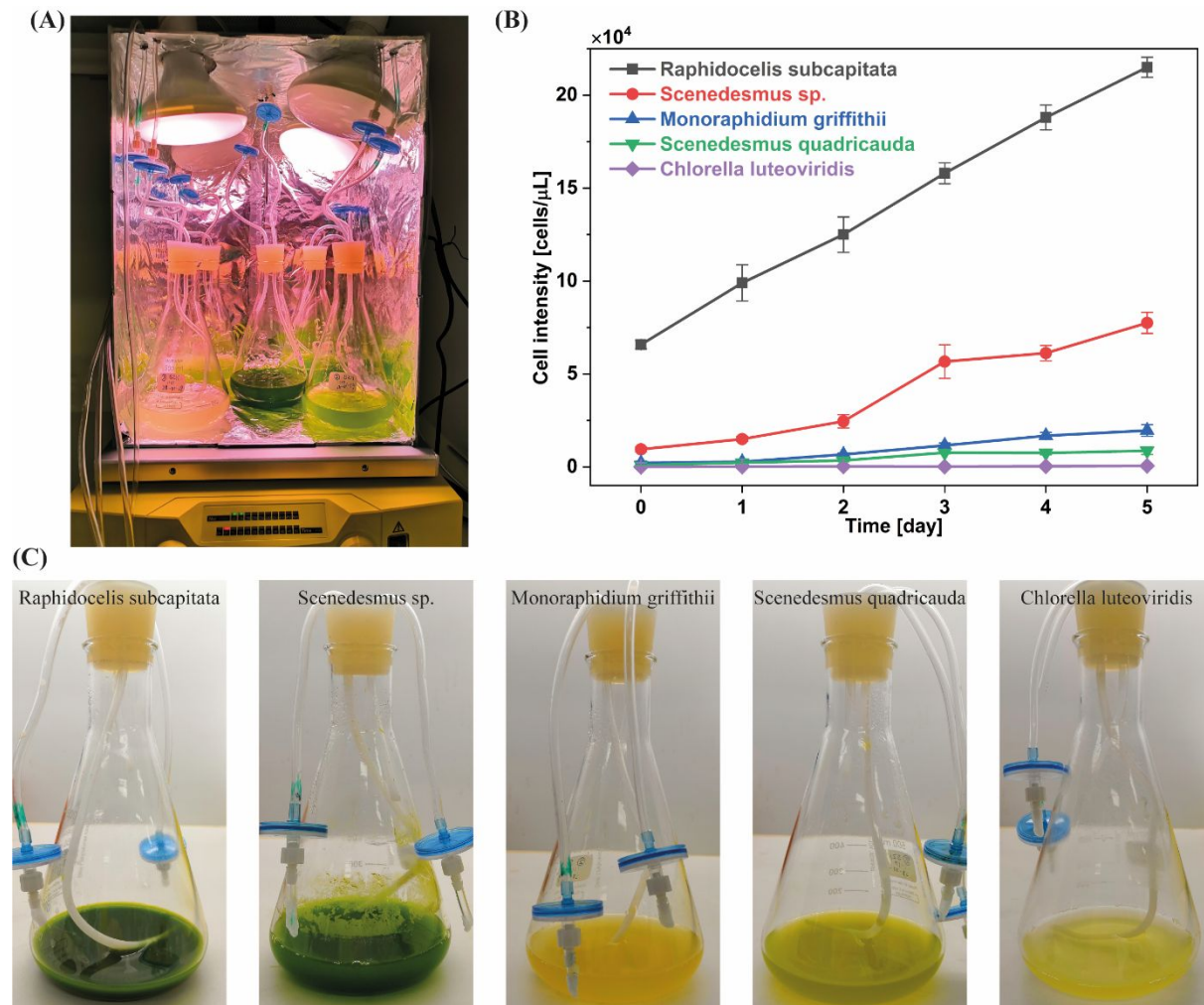


**Figure S1.** (A) A photo of the home-built algae culture system, described in Materials and Methods. (B) Growth curve of the cultured algae over a period of 5 days. The algae were counted using a hemocytometer (Thoma, Paul Marienfeld GmbH & Co. KG). (C) Photos of the five different strains of algae in the culture flask after 1 month of culture, showing that only the *Scenedesmus sp.* create fouling films on the wall of the flask.

## SI 2: Fabrication of magnetic artificial cilia (MAC)

The MAC used in this article are the so-called LAP MAC (MAC with linearly aligned magnetic particles along the cilia's long axis) reported in our previous study.<sup>41</sup> The fabrication process of the MAC can be summarized as follows (**Figure S2**): (1) A mold, featured with an array of microwells of 10×10 rows with the central 4×4=16 microwells “absent”, was fabricated using standard photolithography. (2) A uniform precursor mixture of polydimethylsiloxane (PDMS, Sylgard 184, Dow Corning, Base to Curing Agent weight ratio is 10:1) and superparamagnetic microparticles (Carbonyl iron powder, CIP, 99.5%, SIGMA-ALDRICH) was casted onto the mold, followed by a degassing procedure. The weight ratio between PDMS and CIP was 1:2. (3) The excess magnetic mixture outside the micro-wells was removed. (4) Pure PDMS (Base to Curing Agent weight ratio = 10:1) was casted onto the mold. After degassing the pure PDMS layer was defined to a thickness of 100 μm by spin-coating at a rotating speed of 500 rpm for 50 s. (5) A permanent magnet with a size of 15×15×8 mm<sup>3</sup> and a remnant flux density of 1.2 T was

put underneath the mold in order to align the magnetic particles within the mold. The sample was left in an oven at 80 °C for 3 hours to cure the mixture. (6) The cured pure PDMS layer with PDMS-CIP micropillars was peeled off the mold. Finally, the MAC with the same geometry as the mold, namely a diameter of 50 μm and a height of 350 μm, were obtained (Figure 1A), “standing” on a transparent PDMS base substrate. By fabricating molds featured with microwells of different pitches, MAC with variable pitches of 250, 350, and 450 μm, respectively, were molded. The magnetic properties and the bending performance of the artificial cilia were reported in our earlier paper.<sup>41</sup>

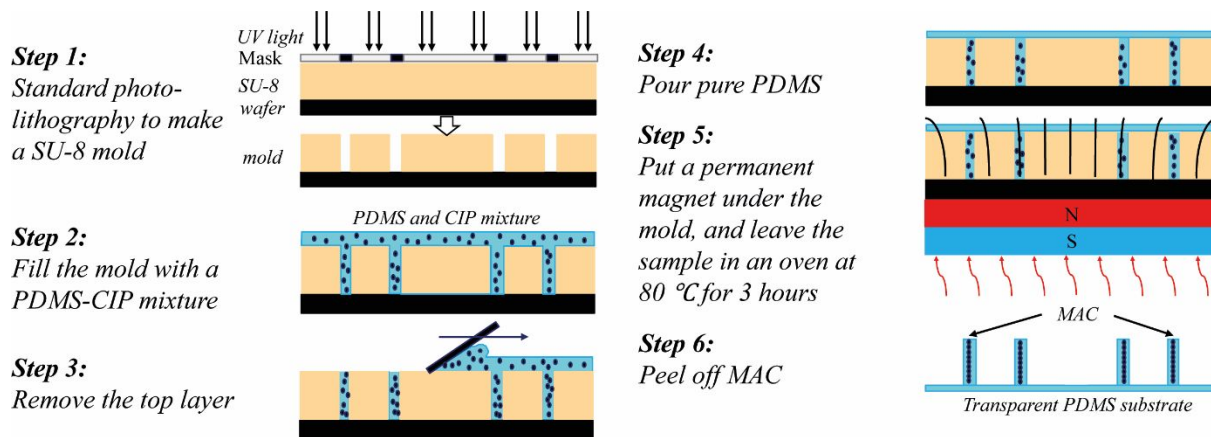


**Figure S2.** Schematics of the fabrication process of the MAC. The illustration is not to scale. Reproduced with permission.<sup>41</sup> Copyright 2018, Elsevier B.V.

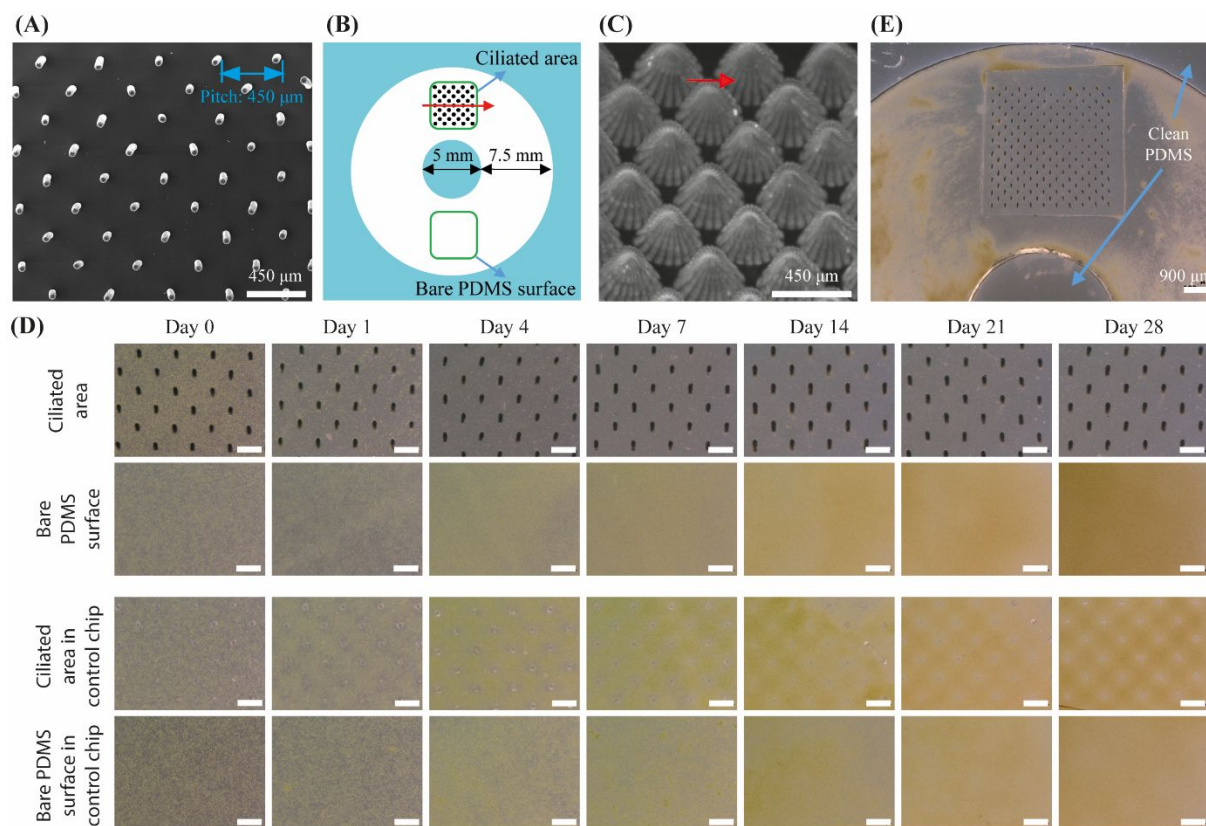
### SI 3: Antifouling efficiency of fully-ciliated surfaces

Figure S3A shows an SEM image of the fully-ciliated surface that is covered with MAC arranged in a staggered configuration with a pitch of 450  $\mu\text{m}$ . The total amount of cilia was 181. The ciliated surface was integrated in a closed circular microfluidic chip with a rectangular cross section with a channel width of 7.5 mm and a channel height of 2 mm (Figure S3B). The chip was filled with algae *Scenedesmus sp.* (Figure 1D) suspended in the culture medium (concentration:  $1 \times 10^4$  cells  $\mu\text{L}^{-1}$ ), see Materials and Methods for details on the algae culture. The MAC were actuated to perform a tilted conical motion (Figure S3C) by a homebuilt magnetic setup (Figure 1G, see Materials and Methods for details) at a constant revolution frequency of 40 Hz. The antifouling results of the fully-ciliated surface are shown in Figure S3D. Figure S3E shows a broader bright-field microscopy image of the experiment after 28 days of actuation. It is clear that the whole ciliated area is almost completely clean after one week of actuation. This is likely because the MAC motion-generated hydrodynamic shear forces are strong enough to overcome

the adhesive strength between the algae and the PDMS surface. Specifically, when the MAC sweep close to the PDMS substrate (during the recovery stroke) the MAC can generate substantial local flow in the ciliated area with a maximal speed of approximately  $6 \times 10^4 \mu\text{m s}^{-1}$  (the maximal speed of the cilia tip during the recovery stroke).<sup>41</sup> This is one order of magnitude larger than the local flow within the central unciliated area (Figure 4B), and two orders of magnitude larger than the global flow in the chip (Figure 4C); and it can impose stronger shear forces on the algae lying on the bottom of the channel (i.e., on the substrate).

Based on the findings in our earlier work,<sup>40</sup> we speculate that the fully-ciliated surface is able to remove and/or exclude larger micro-fouling agents than we used here (12  $\mu\text{m}$  in average) as well as macro-fouling agents.





**Figure S3.** The antifouling capability of the fully-ciliated surfaces. (A) A top-view SEM image of the fully ciliated surface covered with MAC arranged in a staggered configuration. The MAC have a pitch of  $450\ \mu\text{m}$ . The total amount of cilia is 181. (B) Schematic drawing of the circular microfluidic chip integrated with the “fully-ciliated surface”, indicating the location of the ciliated surface area and the observation areas. The height of the chip is 2 mm. The red arrow denotes the direction of the effective stroke of the cilia motion. (C) A top-view image of the motion of the rotating MAC at 40 Hz in water. The image is composed of 25 overlapping frames in one actuation cycle. The red

arrow indicates the direction of the effective stroke. (D) Bright-field microscopy images of one recorded antifouling experiment (top two rows) and one control experiment (bottom two rows) of the fully ciliated surface over a period of 28 days. All scale bars are 300  $\mu\text{m}$ .

(E) A broader bright-field microscopy image of the antifouling experiment with the fully ciliated area after 28 days, showing that the fully ciliated area is almost perfectly clean from a comparison with the clean PDMS part. In the bright-field images, the green dots are the algae, and the color of clean PDMS is grey.

#### SI 4: Antifouling efficiency of partially-ciliated surfaces

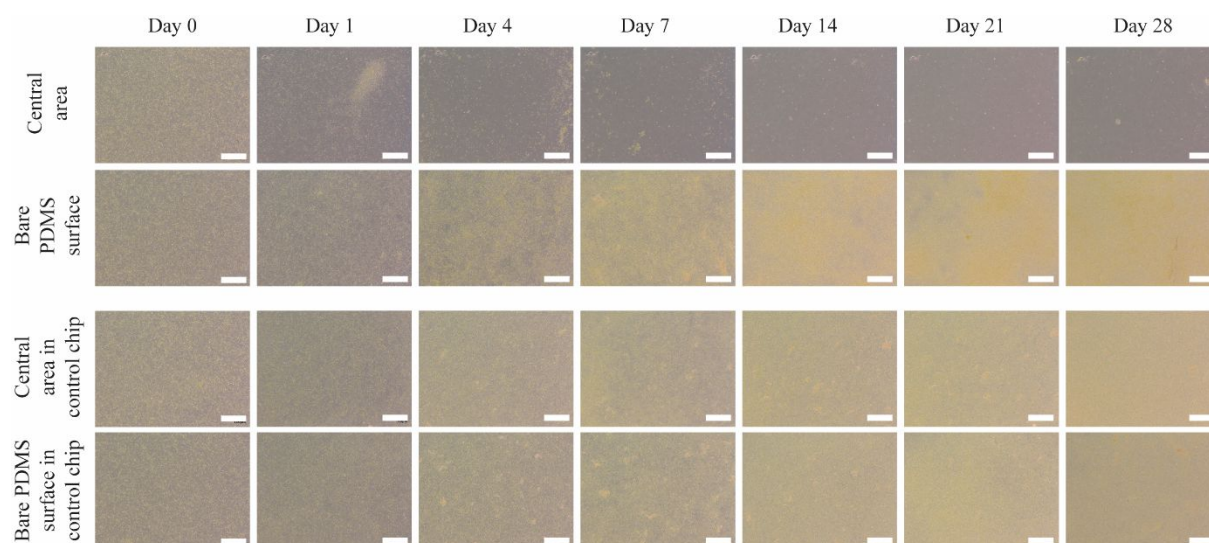
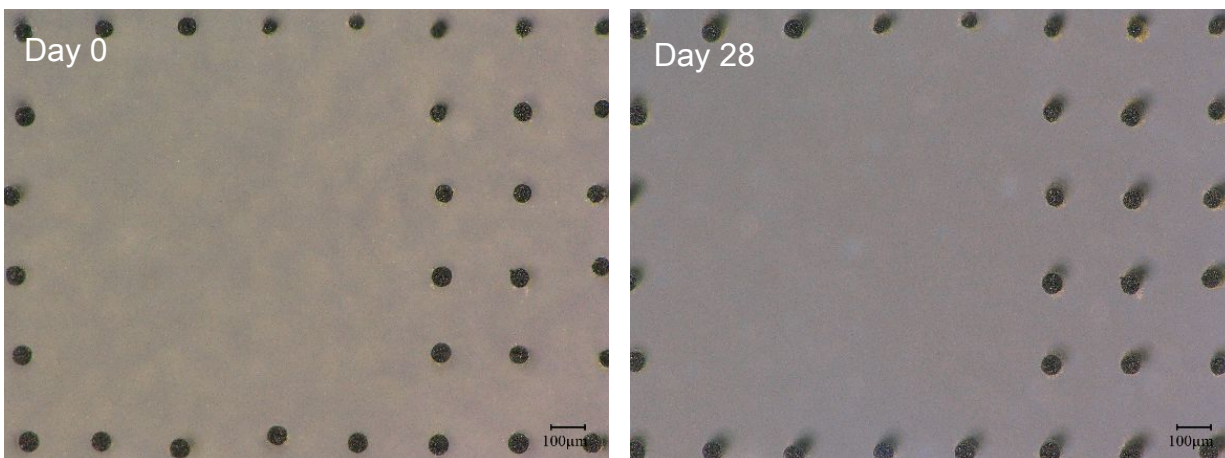


*Figure S4. Bright-field microscopy images of one recorded antifouling experiment at the observation areas indicated in Figure 1C, over a period of 28 days, corresponding to the*



*fluorescent images in Figure 2. The MAC have a pitch of 450  $\mu\text{m}$ . All scale bars are 300  $\mu\text{m}$ .*

*Figure S5. Bright-field microscopy images of the MAC with a pitch of 250  $\mu\text{m}$  before actuation and after 28 days of actuation from one representative experiment, showing that the MAC are intact after long-term operation and that few algae adhere to the body surface of the cilia.*

## SI 5: Calculation of the hydrodynamic shear force acting on the algae

The hydrodynamic shear force applying on an alga was approximated by the following equation:

$$F = \tau A = \mu A \frac{dv}{dy}$$

where  $\tau$  is the hydrodynamic shear stress,  $A$  is the cross section area of the alga (which was measured to be  $60 \times 10^{-12} \text{ m}^2$  using ImageJ),  $\mu$  is the dynamic viscosity of the medium (here we assumed it is the same as that of water, which is  $8.9 \times 10^{-4} \text{ Pa}\cdot\text{s}$ ),  $v$  is the horizontal velocity of the generated flow by the MAC motion, and  $y$  is the height above the substrate. We simply assumed that the local flow speed  $v$  was proportional to the height  $y$ , close to the surface. Since the flow generated by the MAC was around  $3 \times 10^3 \mu\text{m s}^{-1}$  at the height of  $6 \mu\text{m}$  as shown in Figure 4B, the local shear rate was  $\gamma = \frac{3 \times 10^3 \mu\text{m s}^{-1}}{6 \mu\text{m}}$

$= 5 \times 10^2 \text{ s}^{-1}$ , the shear stress was  $\tau = (8.9 \times 10^{-4} \text{ Pa}\cdot\text{s}) \cdot 5 \times 10^2 \text{ s}^{-1} = 0.4 \text{ Pa}$ , and the force acting on an algae was  $F = (8.9 \times 10^{-4} \text{ Pa}\cdot\text{s}) \cdot (60 \times 10^{-12} \text{ m}^2) \cdot \frac{3 \times 10^3 \mu\text{m s}^{-1}}{6 \mu\text{m}} \approx 30 \text{ pN}$ .

In typical microfluidic applications in which aqueous fluids are driven by conventional syringe pumps, and with a characteristic cross-sectional dimension of  $100 \mu\text{m}$  and a

characteristic mean velocity of  $1 \text{ mm s}^{-1}$ , the wall shear stress is an order of magnitude smaller. For example, assuming Poiseuille flow in a channel with a circular cross section (with radius  $a = 100 \times 10^{-6}$ ) and with a mean velocity  $\langle v \rangle = 1 \times 10^{-3} \text{ m}\cdot\text{s}^{-1}$ , the wall shear

stress is  $\tau = \frac{4\mu\langle v \rangle}{a} = \frac{4(8.9 \times 10^{-4} \text{ Pa}\cdot\text{s}) \cdot (1 \times 10^{-3} \text{ m}\cdot\text{s}^{-1})}{100 \times 10^{-6} \text{ m}} = 0.04 \text{ Pa}$ .

**SI 6: Self-cleaning efficiency of partially-ciliated surfaces**

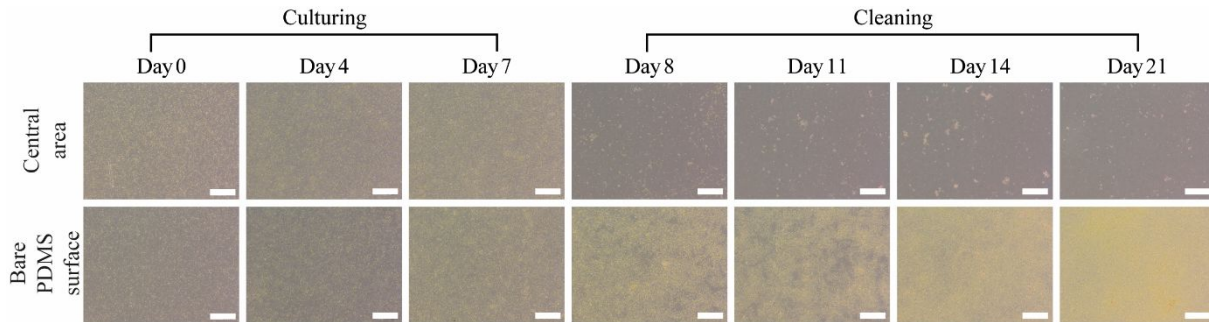


**Figure S6.** Bright-field microscopy images of one recorded self-cleaning experiment at the observation areas indicated in Figure 1C, over a period of 21 days, corresponding to the fluorescent images in Figure 6. The MAC have a pitch of  $450 \mu\text{m}$ . All scale bars are  $300 \mu\text{m}$ . In the bright-field images, the green dots are the algae, and the color of clean PDMS is grey.

## SI 7: Self-cleaning efficiency of partially-ciliated surfaces at a periodical actuation mode

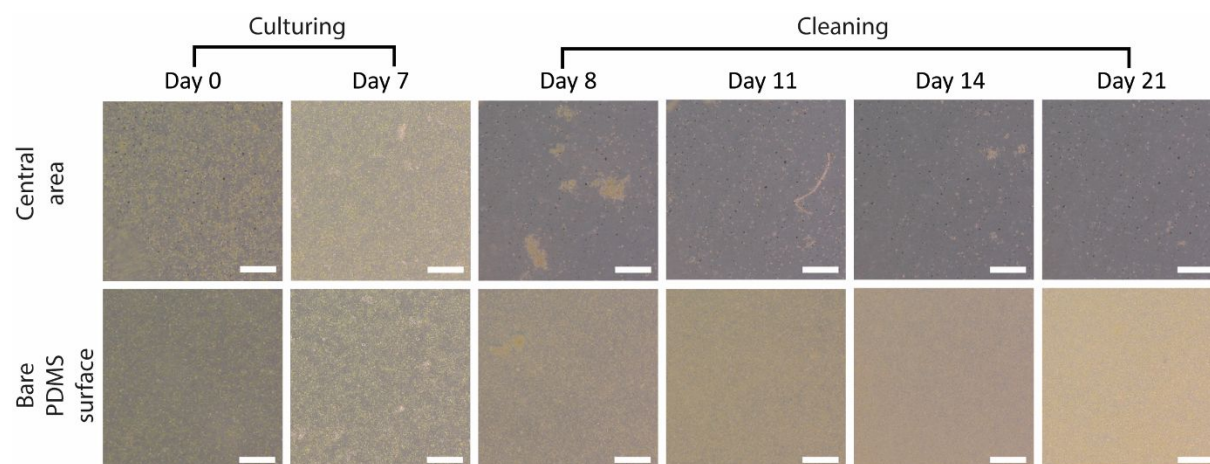


**Figure S7.** Bright-field microscopy images of one recorded self-cleaning experiment of the partially-ciliated surfaces at a periodical actuation mode, at the observation areas indicated in Figure 1C, over a period of 21 days with a 16 hours on / 8 hours off duty cycle. The MAC have a pitch of 250  $\mu\text{m}$ . All scale bars are 200  $\mu\text{m}$ . The green dots are the algae, and the color of clean PDMS is grey.

## SI 8: Verification of the image processing method

**Figure S7** shows a typical comparison between an original microscopy image and the processed image using the method mentioned in the *Materials and Methods* section in the main text. It is clear that the processed image captures almost all the main characteristics of the distribution of algae in the original image, which proves the credibility of the processing method.

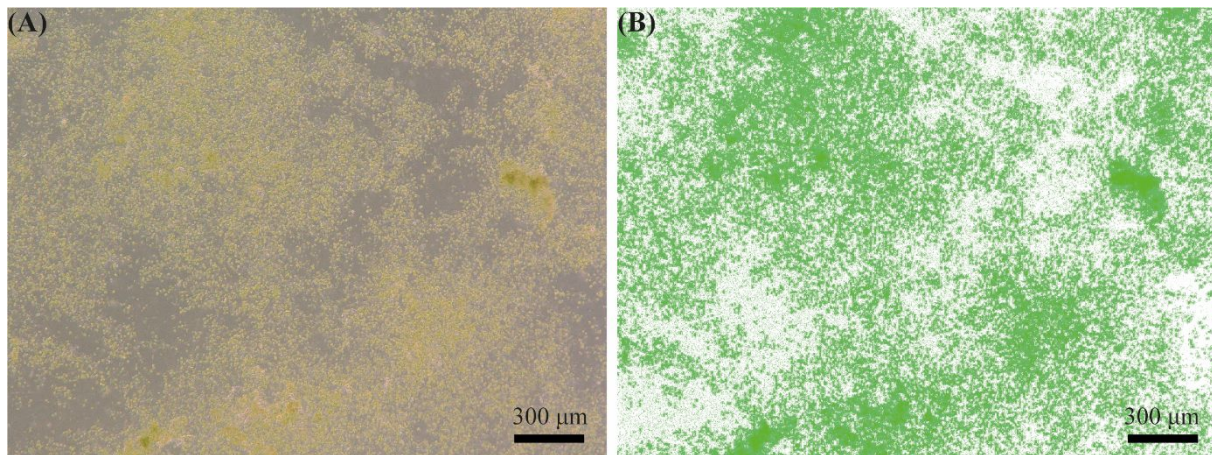


**Figure S8.** Comparison between (A) an original bright-field microscopy image and (B) the corresponding processed image obtained using the method mentioned in the *Materials and Methods* section in the main text. The original image is a bright-field microscopy image of one recorded antifouling experiment at the bare PDMS area in the ciliated chip after 7 days of actuation. The MAC have a pitch of 350 μm.

## SI 9: Supplementary material captions

All experimental movies were recorded using a high-speed camera (Phantom V9) mounted a stereo microscope (Olympus SZ61). The magnetic artificial cilia (MAC) in the movies have a diameter of 50  $\mu\text{m}$ , a height of 350  $\mu\text{m}$  and a pitch of 350  $\mu\text{m}$ , and they perform the tilted conical motion as shown in Figure 1 E and F. The white particles are 12  $\mu\text{m}$  polystyrene tracer particles (micromod Partikeltechnologie GmbH).

**Movie ESI 1** A high-speed video showing the cilia motion generated flow on the PDMS substrate surface in the central unciliated area as shown in Figure 1C. The progressive lines with numbers (1 to 8) at the head show individual trajectories of the traced particles, which also indicate the locations of the measured flow plotted in Figure 4B. Since the camera was focusing on the PDMS substrate, thus the height of the measured flow equals the radius of the tracer particles, which is 6  $\mu\text{m}$ .

**Movie ESI 2** A high-speed video showing the flow generated by the MAC both in and out of the ciliated area.



**Movie ESI 3** A high-speed video showing the cilia motion generated global flow in the bare PDMS area as shown in Figure 1C. The progressive lines are the trajectories of the traced particles at the geometric center (i.e. at the height of 1 mm) of the channel.

**ESI 4** The in-house developed algorithms used in this article to quantitatively analyze the obtained microscopy images. For both the bright-field and fluorescent images, there are three MATLAB codes named *ArtificialCilia*, *CleanIndex* and *ScreenedImage*, respectively. Only the code named *ArtificialCilia* need to be run. There are also a group of images for each type of image enclosed in the same folder as examples to show how the codes work.